eNeuro

Research Article: New Research | Sensory and Motor Systems

An indirect pathway from the rat interstitial nucleus of Cajal to the vestibulocerebellum involved in vertical gaze holding

https://doi.org/10.1523/ENEURO.0294-24.2024

Received: 2 July 2024
Accepted: 19 October 2024

An indirect pathway from the rat interstitial nucleus of Cajal to the vestibulocerebellum involved in vertical gaze holding

Abbreviated title: Neural pathway from the INC to vestibulocerebellum

Taketoshi Sugimura[1], Toshio Miyashita[2,3], Mariko Yamamoto[2], Kenta Kobayashi[4], Yumiko Yoshimura[2] and Yasuhiko Saito[1]

[1]Department of Neurophysiology, Nara Medical University, Kashihara, Nara 634-8521, Japan.

[2]Division of Visual Information Processing, National Institute for Physiological Sciences and School of Life Science, The Graduate University for Advanced Studies (SOKENDAI), Okazaki, Aichi 444-8585, Japan

[3]Department of Anatomy, Teikyo University School of Medicine, 2-11-1, Kaga, Itabashi, Tokyo, 173-8605, Japan

[4]Section of Viral Vector Development, National Institute for Physiological Sciences and School of Life Science, The Graduate University for Advanced Studies (SOKENDAI), Okazaki, Aichi 444-8585, Japan

Author Contributions

T.S. and Y.S. designed research; T.S., T.M., M.Y. and K.K. performed research; T.S. analyzed data; T.S., Y.Y. and Y.S. wrote the paper.

Corresponding author: Yasuhiko Saito, Ph.D.
Department of Neurophysiology, Nara Medical University,
840 Shijo-cho, Kashihara, Nara 634-8521, JAPAN
Tel.: +81-744-29-8827, Fax: +81-744-29-0306
E-mail: syasu@naramed-u.ac.jp

Number of Figures: 7

(Abstract: 230 words, Significance Statement: 112 words, Introduction: 501 words, Discussion: 1058 words)

Acknowledgments: We thank the members of our laboratory for their technical assistance and comments. We also thank the staff of the Institutes of Experimental Animal Research at Nara Medical University for their technical support.

Conflicts of Interest: The authors declare that they have no competing financial interests.

Funding sources: This study was supported by Grants-in-Aid for Scientific Research from the Japan Society for the Promotion of Science (22K15229 to T.S.) and the Cooperative Study Program (22NIPS126, 23NIPS125) of the National Institute for Physiological Sciences.

Abstract

The neural network, including the interstitial nucleus of Cajal (INC), functions as an oculomotor neural integrator involved in the control of vertical gaze holding. Impairment of the vestibulocerebellum (VC), including the flocculus (FL), has been shown to affect vertical gaze holding, indicating that the INC cooperates with the VC in controlling this function. However, a network between the INC and VC has not been identified. In this study, we aimed to obtain anatomical evidence of a neural pathway from the INC to the VC (the INC-VC pathway) in rats. Injection of dextran-conjugated Alexa 488 or adeno-associated virus 2-retro (AAV2retro) expressing GFP into the FL or another VC region (uvula/nodulus) did not reveal any retrogradely labeled neurons in the INC, suggesting that INC neurons do not project directly to the VC. Rabies virus-based transsynaptic tracing experiments revealed that the INC-VC pathway is mediated via synaptic connections with the prepositus hypoglossi nucleus (PHN) and medial vestibular nucleus (MVN). The INC neurons in the INC-VC pathway were mainly localized bilaterally within the rostral region of the INC. Transsynaptic tracing experiments involving the INC-FL pathway revealed that INC neurons connected to the FL via the bilateral PHN and MVN. These results indicate that the INC-VC pathway is not a direct pathway

but is mediated via the PHN and MVN. These findings can provide clues for understanding the network mechanisms responsible for vertical gaze holding.

Significance Statement

Gaze holding is crucial for achieving clear vision. However, the mechanism underlying vertical gaze holding is not fully understood owing to our limited knowledge of the neural connections between the interstitial nucleus of Cajal (INC) and the vestibulocerebellum (VC). In this study, we aimed to identify the neural pathway from the INC to the VC. Retrograde tract-tracing experiments using tracers and viruses revealed that INC neurons do not directly project to the VC; rather, the pathway from the INC to the VC is mediated via synaptic connections with the PHN and MVN. This finding clarifies a new indirect pathway from the INC to the VC that is responsible for vertical gaze holding.

Introduction

During gaze holding, tonic contraction of the extraocular muscles is required to maintain eccentric eye positions against forces that pull the eyes back to the central position. Sustained neural activity for this tonic contraction is produced

through the oculomotor neural integrator, which converts transient burst signals proportional to eye or head velocity into sustained signals proportional to eye position (Skavenski and Robinson, 1973; Robinson, 1975, 1989; Fukushima, 1987, 1991; Fukushima et al., 1992; Fukushima and Kaneko, 1995; Moschovakis, 1997; Leigh and Zee, 2015). The prepositus hypoglossi nucleus (PHN) and the interstitial nucleus of Cajal (INC) are involved in the integrators responsible for horizontal and vertical gaze holdings, respectively (Fukushima, 1987, 1991; Fukushima et al., 1992; Fukushima and Kaneko, 1995; Moschovakis, 1997; Leigh and Zee, 2015).

Previous studies have indicated that the neural mechanisms underlying signal transformation in neural integrators involve the vestibulocerebellum (VC) network (Robinson, 1974; Zee et al., 1981; Godaux and Vanderkelen, 1984; Kheradmand and Zee, 2011; Leigh and Zee, 2015; Beh et al., 2017; Shadmehr, 2017; Shemesh and Zee, 2019) as well as excitatory networks within integrators (Saito and Yanagawa, 2010; Leigh and Zee, 2015; Saito et al., 2017; Saito and Sugimura, 2020) and cholinergic and monoaminergic modulations (Navarro-López et al., 2004, 2005; Zhang et al., 2016, 2018; Saito and Sugimura, 2023). It

is difficult for the PHN alone or the INC alone to produce a sufficient time constant for achieving gaze holding; rather, the neural networks, including these neural nuclei and the VC, may extend this time constant (Robinson, 1974; Kamath and Keller, 1976; Zee et al., 1980, 1981; Kheradmand and Zee, 2011; Leigh and Zee, 2015). Indeed, cerebellectomy or a local lesion within the VC, including in the cerebellar flocculus (FL), results in impaired horizontal and vertical gaze holding (Robinson, 1974; Zee et al., 1981; Godaux and Vanderkelen, 1984), causing the eyes to drift back toward the primary position. Therefore, it is important to identify the neural networks both between the PHN and VC and between the INC and VC to elucidate the mechanisms by which gaze holding is controlled (Zee et al., 1980, 1981; Kheradmand and Zee, 2011; Leigh and Zee, 2015; Bertolini et al., 2019).

Projections from the PHN to the VC have been demonstrated in various experimental animals (Blanks et al., 1983; Sato et al., 1983; Langer et al., 1985; Blanks, 1990; McCrea and Horn, 2006), and cholinergic neurons in the PHN have also been shown to project to various cerebellar regions, including the VC (Barmack et al., 1992b, 1992a; Zhang et al., 2014; Sugimura and Saito, 2021). In contrast to the PHN-VC pathway, only one report—conducted in cats—has

identified extremely sparse projections from the INC to the VC (Røste and Dietrichs, 1988). This finding suggests that the INC does not significantly interact with the VC; however, lesions within the VC have been shown to affect vertical gaze holding (Zee et al., 1981). Therefore, in this study, we aimed to obtain anatomical evidence of an INC-VC pathway via rabies virus-based transsynaptic tracing.

Materials and Methods

All experimental procedures were approved by the Animal Care Committee of Nara Medical University and the Experimental Animal Committee of the National Institute for Physiological Sciences. The experiments were carried out in accordance with the guidelines outlined by the U.S. National Institutes of Health regarding the care and use of animals for experimental research. A total of 15 male Long–Evans rats were used in this study. Tracer and AAV injections were performed in rats aged 7–8 postnatal weeks.

Tracer injection

137 The tracer injection methods used were similar to those described previously
138 (Sugimura and Saito, 2021). Dextran-conjugated Alexa 488 (5% in Tris-buffered
139 saline, Invitrogen/Thermo Fisher Scientific) was injected into the FL, uvula and
140 nodulus (UN), lobules Ⅰ-Ⅱ in the vermis and crus Ⅰ-Ⅱ. The tracers were
141 injected unilaterally into the right FL and crus Ⅰ-Ⅱ and into the midline regions
142 of the UN and lobules Ⅰ-Ⅱ in the vermis. Under inhalation anesthesia with 2–
143 3% isoflurane, the rats were placed in a stereotaxic apparatus. Using a dental
144 drill, a small hole was drilled in the cranium over the paraflocculer lobe, the
145 midline region of the posterior vermis, the midline region of the anterior vermis,
146 or the posterior hemisphere for tracer injection into the FL, UN, lobules Ⅰ-Ⅱ, or
147 crus Ⅰ-Ⅱ, respectively. A glass micropipette with a tip diameter of 40–60 μm
148 was connected to a Hamilton syringe with polyethylene tubing and filled with oil.
149 Dextran-conjugated Alexa 488 was drawn into the tip of the micropipette. For
150 injection into the FL, the tip of the micropipette was introduced horizontally, 20°
151 posterior to the mediolateral axis, and inserted 2.7 mm beneath the surface to
152 pass through the paraflocculer lobe and enter the FL. For the injections into the
153 other three regions, the tip was positioned on the midline, 4.8 mm posterior to
154 lambda, at a depth of 4.8 mm for the UN; on the midline, 1.0 mm posterior to

lambda, at a depth of 4.8 mm for lobules Ⅰ-Ⅱ in the vermis; and 4.5 mm lateral to the midline, 5.0 mm posterior to lambda, at a depth of 1.2 mm for crus Ⅰ-Ⅱ. Tracer injection was performed by applying pressure for more than 5 min per site. The tracer was injected at two sites in the FL and at one site in the other region. After the injection of a total of 0.8–1.0 μL of tracer per rat, the pipette was maintained at its position for 5 min before withdrawal. Following incision suturing, an antibiotic (gentamicin ointment; MSD, Tokyo, Japan) was applied to the wound, and a nonsteroidal anti-inflammatory drug (flunixin meglumine, 1.5 mg/kg; Sigma–Aldrich, St. Louis, MO) was applied subcutaneously.

Virus preparation and virus injection for transsynaptic tracing

The glycoprotein (G)-deleted rabies virus pseudotyped with avian sarcoma leucosis virus envelope protein (EnvA), EnvA-HEP-ΔG-mCherry, was produced as previously described (Osakada and Callaway, 2013; Mori and Morimoto, 2014) with minor modifications. First, to obtain the G-deleted rabies virus HEP strain, BHK-T7/9 cells were transfected with plasmids encoding the entire rabies virus genome with mCherry instead of rabies glycoprotein (pcDNA-HEP-ΔG-mCherry) and helper plasmids encoding the rabies nucleoprotein (RN; pcDNA-

RN), phosphoprotein (RP; pcDNA-RP), and polymerase (RL; pcDNA-RL) genes using TransIT-LT1 reagent (Takara Bio), as described in the manufacturer's instructions. Once the mCherry fluorescence signal increased, the culture medium containing the rabies virus HEP-ΔG-mCherry was collected and transferred to the BHK-21 cell line expressing the SADcvsG glycoprotein to increase the titer and amount of HEP-ΔG-mCherry virus. Second, the BHK-21 cell line expressing EnvA was infected with the collected HEP-ΔG-mCherry virus. Because HEP-ΔG-mCherry lacks glycoprotein in the genome, the culture media contained the pseudotyped rabies virus EnvA-HEP-ΔG-mCherry. The virus was concentrated via centrifugation of the culture medium. We obtained the EnvA-HEP-ΔG-mCherry (referred to in the text as EnvA-RVdG-RFP) virus with an infectious titer of 2.3×10^8 IU/ml in HEK293-TVA (tumor virus receptor A) cells. Retrograde AAVs were used to express rabies G and TVA for rabies virus tracing in an axonal projection area-specific manner. The sequence between the two loxP sites of the FLEX plasmids, pAAV-CA-FLEX-SADcvsG and pAAV-EF1α-FLEX-GT (Addgene plasmid #26198), was inverted by Cre recombinase (M0298, New England Biolabs) in vitro. The modified plasmids pAAV-CA-SADcvsG and pAAV-EF1α-GT were used to produce retrograde AAV vectors (AAV2retro-CA-

191 SADcvsG and AAV2retro-EF1α-GFP-TVA). The titers of AAV2retro-CA-
192 SADcvsG (referred to in the text as AAV2retro-G) and AAV2retro-EF1α-GFP-
193 TVA (referred to in the text as AAV2retro-GFP-TVA) were 2.0×10^{12} genomic
194 copies (GC)/ml and 9.8×10^{11} GC/ml, respectively. In this study, AAV2retro-G and
195 AAV2retro-GFP-TVA are referred to as helper AAV2retro viruses.
196
197 For transsynaptic labeling, a total of 1.0 µl of a 1:1 mixture of AAV2retro-GFP-
198 TVA and AAV2retro-G was injected into the right FL (0.5 µl into each of the two
199 sites) or into the midline region of the UN (1.0 µl into a single site). Three weeks
200 later, 0.8 µl of EnvA-RVdG-RFP was injected unilaterally into the right (Figures 3,
201 4 and 5) or left (Figure 6) PHN and medial vestibular nucleus (MVN). Injection
202 into only the PHN and MVN was considered difficult because the two nuclei are
203 located adjacent to each other; therefore, the virus was injected into both the PHN
204 and MVN. The tip was positioned 0.5–1.0 mm lateral to the midline, 3.8 mm
205 posterior to lambda, at a depth of 6.5 mm from the surface of the cerebellum for
206 injection into the PHN and MVN. The virus was pressure injected via the same
207 procedure used for the tracer injection. Five days after the injection, the cells were

maintained to allow infection with EnvA-RVdG-RFP, transsynaptic spread of the virus, and sufficient RFP expression for labeling presynaptic neurons.

Histological procedures

Three to five days after tracer injection or five days after rabies virus injection, the rats were anesthetized via isoflurane inhalation followed by intraperitoneal injection of a mixture of medetomidine (0.15 mg/kg), midazolam (2.0 mg/kg), or butorphanol (2.5 mg/kg). The rats were then transcardially perfused with 0.01 M phosphate-buffered saline (PBS, pH 7.4), followed by 4% paraformaldehyde in 0.1 M phosphate buffer. The brain was removed and postfixed in the same fixative for one day. The injection sites and the brain areas were cut frontally into 60 µm sections via a microslicer (Dosaka EM). For the tracer experiments, some slices were counterstained with red fluorescent Nissl stain (1:200, NeuroTrace 530/615; Thermo Fisher Scientific, Waltham, MA, USA). For transsynaptic tracing, to enhance GFP signals, the sections were incubated overnight at room temperature with chicken IgY anti-GFP antibody (1:1000; ab13970, Abcam) in PBS containing 5% bovine serum albumin, 0.1% Triton X-100, and 0.1% NaN_3, followed by Alexa Fluor 488 goat anti-chicken IgY (1:400; ab150169, Abcam) in

the same solution at room temperature for 2 h. The sections were mounted on MAS-coated slides (Matsunami Glass) using antifade medium (ProLong Gold Antifade Reagent, Invitrogen) or a DAPI-containing fluoromount (DAPI Fluoromount-G, Southern Biotech, 0100-20).

Observation and data analysis

Images of the brain sections were captured under a laser-scanning confocal microscope (C2+, Nikon) or a fluorescence microscope (BZ-X710, Keyence). The images were then processed and analyzed via FIJI (Schindelin et al., 2012). For the tracer experiments of the INC, every other 60 µm coronal section from bregma -5.04 mm to -6.84 mm was investigated. For transsynaptic tracing, every other 60 µm coronal section was investigated from bregma -10.32 mm to -12.84 mm for the PHN, from bregma -9.96 mm to -13.08 mm for the MVN, and from bregma -5.04 mm to -6.84 mm for the INC; all coordinates were determined according to the rat brain atlas (Paxinos and Watson, 2018). To determine whether the number of RFP-expressing neurons demonstrated a rostrocaudal gradient within the INC, we separated the INC into rostral, intermediate, and caudal parts. Each of the parts, consisting of five alternating sections, was 600 µm in length in the

244 rostrocaudal direction. GFP- or RFP-expressing neurons were manually counted
245 via the cell counter plugin in FIJI. The detection threshold for GFP- or RFP-
246 labeled neurons was arbitrarily defined. Neurons labeled with both GFP and RFP
247 were selected from neurons that showed positive fluorescence in both the RFP
248 and the GFP fluorescence images. For transsynaptic tracing, cell counts were
249 performed for the PHN and MVN ipsilateral to the site of rabies virus injection to
250 identify starter neurons that expressed both GFP and RFP and in the bilateral
251 INC to identify RFP-expressing neurons. All values are shown as the
252 means ± SDs, and the error bars in the figures represent the SDs. Unless
253 otherwise noted, the number (n) refers to the number of rats analyzed. Statistical
254 analysis was performed via the Wilcoxon signed-rank test or repeated-measures
255 one-way ANOVA followed by the Tukey–Kramer test for multiple comparisons,
256 for which an adjusted p value was calculated. The normality of the data was
257 determined via the Shapiro–Wilk test. Differences in variance among the groups
258 were assessed via the Brown–Forsythe test. The analyses were performed via
259 GraphPad Prism 8 (GraphPad Software, San Diego, CA). The threshold for
260 statistical significance was defined as $p < .05$.
261

Results

INC neurons do not project directly to the VC

To investigate the INC-VC pathway, we injected dextran-conjugated Alexa 488 into two distinct regions of the VC, the FL (n = 2) and lobules IX and X of the cerebellar vermis (uvula and nodulus, UN) (n = 2) (Figures 1a1, b1). The tracers were widely distributed both mediolaterally and rostrocaudally within the FL and UN (Figures 1a2, b2). Although retrogradely labeled neurons were observed in the PHN (Figures 1a3-4, b3-4), no labeled neurons were observed in the INC (Figures 1a6-7, b6-7). Successful tracer injection was confirmed by observing retrogradely labeled neurons in the rostral part of the medial accessory olive (r-MAO) contralateral to the injection site (Figure 1a5) and in the subnucleus beta of the inferior olive (beta) (Figure 1b5), which are known to project to the FL and UN, respectively (Sugihara and Shinoda, 2004; Sugihara et al., 2004; Ando et al., 2020). These results indicate that INC neurons do not project directly to the FL or UN.

Lobules I-II in the cerebellar vermis and crus I-II in the hemisphere receive vestibular inputs (Kotchabhakdi and Walberg, 1978; Matsushita and Okado,

1981; Hirai, 1983) and inputs from the PHN (Payne, 1983; Belknap and McCrea, 1988; Røste, 1989; Sugimura and Saito, 2021), respectively. Therefore, to determine the possibility that INC neurons project to these cerebellar regions rather than the VC, we injected dextran-conjugated Alexa 488 into lobules I-II in the vermis (n = 2) (Figure 2a1) and into crus I-II (n = 2) (Figure 2b1). The tracers were widely distributed both mediolaterally and rostrocaudally in both lobules I-II (Figure 2a2) and crus I-II (Figure 2b2). Retrogradely labeled neurons were observed in the PHN (Figures 2a3-4, b3-4) but not in the INC (Figures 2a7, b7). We also confirmed retrogradely labeled neurons in the caudal parts of the medial accessory olive (c-MAO), which project to lobules I-II (Sugihara and Shinoda, 2004) (Figure 2a5), and in the ventral lamella of the principal olive (v-PO) and the dorsal lamella of the principal olive (d-PO), which project to crus I-II (Sugihara and Shinoda, 2004) contralateral to the injection site (Figure 2b5). These results indicate that INC neurons directly project neither to the VC nor to lobules I-II and crus I-II.

Indirect pathway from the INC to the VC

297 Based on the results described above and the hypothesis that the INC and the
298 VC constitute an oculomotor neural integrator involved in the control of vertical
299 gaze holding, the pathway from the INC to the VC may involve other areas. The
300 PHN and the MVN receive inputs from the INC (McCrea and Baker, 1985;
301 Belknap and McCrea, 1988; Spence and Saint-Cyr, 1988a, 1988b;
302 Kokkoroyannis et al., 1996) and send outputs to the VC (Zhang et al., 2014; Leigh
303 and Zee, 2015; Sugimura and Saito, 2021). We therefore tested the possibility
304 that the INC-FL and INC-UN pathways are mediated via the PHN and MVN via
305 rabies virus-based transsynaptic tracing (Figure 3a). Precise injections of helper
306 adeno-associated virus 2-retro (AAV2retro) viruses into the right side of the FL (n
307 = 3) (Figure 3b1) or the midline region of the UN (n = 4) (Figure 3c1) confirmed
308 the presence of GFP-expressing neurons in the PHN (Figures 3b2, c2) and the
309 MVN (Figures 3b3, c2). Starter cells, which were initially rabies-infected and
310 expressed both GFP and RFP, were observed in the PHN and MVN (Figures
311 3b2-3, c2), although the number of starter cells observed in the two regions
312 differed among the rats (Figure 3d1). Neurons that expressed RFP alone—those
313 that transsynaptically received retrograde rabies virus infection via starter cells—
314 were observed in the bilateral INCs (Figures 3b4, c3). The number of RFP-

315 expressing neurons in the INC was also different for each rat (Figure 3d2) but
316 was positively correlated with the number of starter cells (R^2 = 0.901, Figure 3d3).
317 INC neurons that expressed GFP alone were not observed, confirming that there
318 were no direct projections from the INC to the FL or UN. These results indicate
319 that the INC-VC pathway functions via synaptic connections with the PHN and
320 MVN.
321
322 In the PHN and MVN, neurons that exhibited RFP alone were also observed
323 (Figures 3b2-3, c2), which could be starter cells that express TVA at levels
324 undetectable via GFP because of strong interactions between the wild-type TVA
325 and EnvA-RVdG (Callaway and Luo, 2015; Kim et al., 2015). We tested this
326 possibility by injecting helper AAV2retro without AAV2retro-G into the UN and
327 EnvA-RVdG-RFP into the PHN and MVN to prevent transsynaptic infection (n =
328 2). All PHN and MVN neurons that expressed RFP expressed GFP (Figure 4).
329 These results indicate that the expression of RFP alone by PHN and MVN
330 neurons resulted from transsynaptic infection of starter cells. These findings
331 suggest that the neurons in the PHN and MVN that express RFP alone are
332 interneurons that form synaptic connections and provide inputs to starter cells.

Distribution of INC neurons that participate in the INC-VC pathway via the PHN and MVN

RFP-expressing neurons were observed in the bilateral INCs, despite the unilateral injection of rabies virus into the PHN and MVN (Figures 3b4, c3). Therefore, the numbers of RFP-expressing neurons in the left and right INCs were compared. The number of RFP-expressing neurons did not significantly differ between the bilateral INCs when the helper AAV2 retrovirus was injected into the UN (ipsilateral: 21 ± 14, contralateral: 27 ± 31, $p > 0.999$, $n = 4$), nor did it significantly differ between the ipsilateral (13 ± 10) and contralateral (21 ± 15) sides when the virus was unilaterally injected into the FL ($p = 0.250$, $n = 3$). In addition to comparing the absolute neuron numbers, we calculated the bias index for each animal to assess laterality via the formula (ipsi−contra)/(ipsi+contra), where “ipsi” and “contra” refer to the number of RFP-expressing neurons in the ipsilateral and contralateral INCs, respectively. The bias index values were -0.020 ± 0.212 for the UN group (Figure 3c, $n = 4$) and -0.275 ± 0.220 for the FL group (Figure 3b, $n = 3$). One-sample t tests indicated that the mean bias indices in both the UN and FL groups did not significantly differ from zero ($p = 0.864$ and $p =$

0.163, respectively). These results suggest that the INC neurons that received transsynaptic infection from starter cells did not show marked laterality.

We next examined the rostrocaudal distribution of RFP-expressing neurons in the INC. RFP-expressing neurons were more frequently observed in the rostral region than in the intermediate and caudal regions following injection into both the FL (Figures 5a1-3) and UN (Figures 5b1-3). Comparisons of RFP-expressing neurons in the three regions relative to the total number of RFP-expressing neurons in the INC revealed that the percentage in the rostral region was significantly greater than that in the intermediate and caudal regions following injection into both the FL ($p = .0398$ and $p = .0002$, respectively, $n = 3$, Figure 5a4) and UN ($p = .0003$ and $p = .0017$, respectively, $n = 4$, Figure 5b4). These results indicate that the distribution of RFP-expressing neurons depends on the rostrocaudal location within the INC.

The INC is connected to the FL via the bilateral PHNs and MVNs

Finally, we investigated whether INC neurons connect to the FL via the unilateral or bilateral PHNs and MVNs. Following AAV2retro-G and AAV2retro-GFP-TVA

injections into the right FL (Figure 6a1) and EnvA-RVdG-RFP injections into the left PHN and MVN in three rats, starter cells were observed in the left PHN and MVN, and RFP-expressing neurons were observed in the bilateral INCs (Figures 6a2-5). Together with the preceding results (Figure 3), these results indicate that INC neurons connect to the FL via the bilateral PHNs and MVNs. Figure 6b summarizes the pathway from the INC to the FL mediated via the PHN and MVN on the basis of our results on retrograde labeled neurons.

Discussion

In this study, we aimed to obtain anatomical evidence of an INC-VC pathway. We did not find that INC neurons directly projected to the FL or UN via retrograde tracing experiments. However, rabies virus-based transsynaptic tracing experiments revealed that INC neurons received retrograde transsynaptic infection with the virus via projection neurons to the FL and UN in the PHN and MVN. These results indicate that the neural pathway from the INC to the VC is formed via synaptic connections with the PHN and MVN.

When dextran-conjugated Alexa 488 or AAV2retro-GFP-TVA was injected into the FL or UN of the rats, no retrogradely labeled neurons were observed in the INC, although many labeled neurons were observed in the PHN (Figures 1 and 3). The cerebellum is composed of a zonal structure with specific input–output relationships as its functional unit. Local stimulation of distinct zones (the H-zone and V-zone) in the FL has been shown to induce horizontal and vertical eye movements in various animals, including rabbits (Dufossé et al., 1977; Nagao et al., 1985), cats (Sato and Kawasaki, 1984, 1990), and monkeys (Balaban and Watanabe, 1984). Further detailed studies in mice and rabbits based on the complex spike modulation of floccular Purkinje cells in response to optokinetic stimulation revealed that the cells in zones 1 and 3 (HA zones) preferentially respond to rotation about the horizontal axis oriented at the 135° ipsilateral azimuth, whereas those in zones 2 and 4 (VA zones) preferentially respond to rotation about the vertical axis (De Zeeuw et al., 1994; Schonewille et al., 2006). Climbing fiber inputs to Purkinje cells in the HA and VA zones originate mainly from neurons in the ventrolateral outgrowth (VLO) and the caudal dorsal cap (CDC) of the contralateral inferior olive, respectively (Tan et al., 1995; Sugihara et al., 2004; Voogd and Wylie, 2004; Schonewille et al.,

404 2006). In the present study, we observed retrogradely GFP-labeled neurons in
405 the contralateral VLO and CDC following injection of helper AAV2 retroinjected
406 into the FL (Figure 7). These findings indicate that the AAV viruses were
407 injected into both the HA and VA zones in the FL and that the absence of
408 retrogradely GFP-labeled neurons in the INC was not due to a failed AAV
409 injection into the HA zones.

410

411 Our transsynaptic tracing experiments using the rabies virus revealed that the
412 INC is connected to both the FL and UN via the PHN and MVN. Although these
413 indirect INC-VC pathways pass through the region of the horizontal integrator,
414 they may play a role in vertical gaze holding. Indeed, previous studies have
415 shown that postaccadic drift appears to be induced during vertical eye
416 movements and that horizontal gaze holding is impaired when the PHN and MVN
417 are chemically lesioned or pharmacologically inactivated (Cannon and Robinson,
418 1987; Kaneko, 1997). The induction of vertical drifts despite the impairment of
419 horizontal integrators may be due to insufficient functioning of the INC-VC
420 pathway via the PHN and MVN. Extracellular-unit spike recording experiments
421 have revealed that some PHN and MVN neurons exhibit tonic activity related to

422 vertical eye position (Baker et al., 1976; Tomlinson and Robinson, 1984),
423 suggesting that these neurons are involved in the indirect INC-VC pathway.
424
425 Our study further clarified the characteristics of the INC-VC pathway. First, INC
426 neurons that participate in the INC-VC pathway are present on both sides of the
427 INC and exhibit no significant laterality (Figure 3). Second, the INC neurons
428 involved in the INC-VC pathway are located mainly in the rostral part of the INC
429 (Figure 5). A previous study on vertical eye movements showed that unilateral
430 injections of a retrograde tracer into the entire vestibular complex result in
431 retrogradely labeled cells in both the ipsilateral and contralateral INCs, largely in
432 their rostral regions (Spence and Saint-Cyr, 1988b). These distributions of INC
433 neurons are similar to our results; therefore, the pathway from the INC to the
434 vestibular nuclei may be common in vertical eye movements and vertical gaze
435 holding. Third, the pathway from the INC to the FL is mediated via both the
436 ipsilateral and contralateral PHNs and MVNs (Figure 6). In our study, virus-
437 infected neurons in the bilateral INCs were observed following unilateral injection
438 of the AAV virus into the FL, suggesting that the pathway from the INC reached
439 the bilateral FLs via the bilateral PHNs and MVNs. Previous studies have shown

that postsaccadic drifts in vertical eye movements are less pronounced in subjects with unilateral PHN and MVN lesions than in those with bilateral lesions (Cannon and Robinson, 1987; Kaneko, 1997). The weaker symptomology experienced in subjects with unilateral lesions of the PHN and MVN may be due to incomplete disruption of the INC-FL pathway, which is mediated via the bilateral PHNs and MVNs.

Cell groups in paramedian tracts (PMTs), which are scattered along the paramedian regions of the pons and medulla, project to the floccular region (Büttner-Ennever et al., 1989; BÜTTNER-ENNEVER and HORN, 1996). All premotor neurons that project to ocular motoneurons send axon collaterals to the PMT (Büttner-Ennever et al., 1989; BÜTTNER-ENNEVER and HORN, 1996). A previous monkey study showed that the INC projects to the PMT (BÜTTNER-ENNEVER and HORN, 1996). Lesions within or inactivation of PMT cell groups lead to downbeat nystagmus (Nakamagoe, 2000; Nakamagoe et al., 2012; Helmchen et al., 2013), upbeat nystagmus (Tian et al., 2023), and omnidirectional gaze-evoked nystagmus (Anagnostou et al., 2009). These findings suggest that the pathway from the INC to the FL via the PMT is involved in vertical gaze

holding. Because some PMT neurons encode activity similar to that of oculomotor neurons, PMT cell groups may send an efferent copy of the motor command to the FL (Cheron et al., 1995; Horn and Leigh, 2011; Leigh and Zee, 2015). The efference copy is used for purposes such as motion prediction rather than for the direct control of eye position. Therefore, the INC-FL pathway via the PMT may not substantially participate in gaze holding. Previous anatomical methods did not clarify how the INC connects to the VC; therefore, the neural networks around the VC in the vertical oculomotor integrator remain unclear. Our present study, which uses the rabies virus-based transsynaptic tracing method, demonstrated that the INC communicates with the VC via the PHN and the MVN. This finding provides clues as to how the INC interacts with the VC and helps gain insights into the network mechanisms responsible for vertical gaze holding.

References

Anagnostou E, Spengos K, Margeti S, Vassilopoulou S, Paraskevas GP, Zis V (2009) Vertical and horizontal integrator failure in a ponto-medullary infarction: A possible role for paramedian tract neurons. J Neurol Sci 280:118–119.

476 Ando T, Ueda M, Luo Y, Sugihara I (2020) Heterogeneous vestibulocerebellar
477 mossy fiber projections revealed by single axon reconstruction in the
478 mouse. J Comp Neurol 528:1775–1802.

479 Baker R, Gresty M, Berthoz A (1976) Neuronal activity in the prepositus
480 hypoglossi nucleus correlated with vertical and horizontal eye movement in
481 the cat. Brain Res 101:366–371.

482 Balaban CD, Watanabe E (1984) Functional representation of eye movements
483 in the flocculus of monkeys (Macaca fuscata). Neurosci Lett 49:199–205.

484 Barmack NH, Baughman RW, Eckenstein FP (1992a) Cholinergic innervation of
485 the cerebellum of the rat by secondary vestibular afferents. Ann N Y Acad
486 Sci 656:566–579.

487 Barmack NH, Baughman RW, Eckenstein FP, Shojaku H (1992b) Secondary
488 vestibular cholinergic projection to the cerebellum of rabbit and rat as
489 revealed by choline acetyltransferase immunohistochemistry, retrograde
490 and orthograde tracers. J Comp Neurol 317:250–270.

491 Beh SC, Frohman TC, Frohman EM (2017) Cerebellar Control of Eye
492 Movements. J Neuro-Ophthalmology 37:87–98.

493 Belknap DB, McCrea RA (1988) Anatomical connections of the prepositus and
494 abducens nuclei in the squirrel monkey. J Comp Neurol 268:13–28.

495 Bertolini G, Romano F, Feddermann-Demont N, Straumann D, Tarnutzer AA,
496 Ramat S (2019) Non-linearity in gaze holding: Experimental results and
497 possible mechanisms, 1st ed. Elsevier B.V.

498 Blanks RHI (1990) Afferents to the cerebellar flocculus in cat with special
499 reference to pathways conveying vestibular, visual (optokinetic) and
500 oculomotor signals. J Neurocytol 19:628–642.

501 Blanks RHI, Precht W, Torigoe Y (1983) Afferent projections to the cerebellar
502 flocculus in the pigmented rat demonstrated by retrograde transport of
503 horseradish peroxidase. Exp Brain Res 52:293–306.

504 BÜTTNER-ENNEVER JA, HORN AKE (1996) Pathways from Cell Groups of
505 the Paramedian Tracts to the Floccular Region. Ann N Y Acad Sci
506 781:532–540.

507 Büttner-Ennever JA, Horn AKE, Schmidtke K (1989) Cell groups of the medial
508 longitudinal fasciculus and paramedian tracts. Rev Neurol (Paris) 145:533–
509 539.

510 Callaway EM, Luo L (2015) Monosynaptic Circuit Tracing with Glycoprotein-
511 Deleted Rabies Viruses. J Neurosci 35:8979–8985.

512 Cannon SC, Robinson DA (1987) Loss of the neural integrator of the
513 oculomotor system from brain stem lesions in monkey. J Neurophysiol
514 57:1383–1409.

515 Cheron G, Saussez S, Gerrits N, Godaux E (1995) Existence in the nucleus
516 incertus of the cat of horizontal-eye-movement-related neurons projecting
517 to the cerebellar flocculus. J Neurophysiol 74:1367–1372.

518 De Zeeuw CI, Wylie DR, Digiorgi PL, Simpson JI (1994) Projections of
519 individual purkinje cells of identified zones in the flocculus to the vestibular
520 and cerebellar nuclei in the rabbit. J Comp Neurol 349:428–447.

521 Dufossé M, Ito M, Miyashita Y (1977) Functional localization in the rabbit's
522 cerebellar flocculus determined in relationship with eye movements.
523 Neurosci Lett 5:273–277.

524 Fukushima K (1987) The interstitial nucleus of Cajal and its role in the control of
525 movements of head and eyes. Prog Neurobiol 29:107–192.

526 Fukushima K (1991) The interstitial nucleus of Cajal in the midbrain reticular
527 formation and vertical eye movement. Neurosci Res 10:159–187.

528 Fukushima K, Kaneko CRS (1995) Vestibular integrators in the oculomotor
529 system. Neurosci Res 22:249–258.

530 Fukushima K, Kaneko CRS, Fuchs AF (1992) The neuronal substrate of
531 integration in the oculomotor system. Prog Neurobiol 39:609–639.

532 Godaux E, Vanderkelen B (1984) Vestibulo-ocular reflex, optokinetic response
533 and their interactions in the cerebellectomized cat. J Physiol 346:155–170.

534 Helmchen C, Glasauer S, Sprenger A (2013) Inverse eye position dependency
535 of downbeat nystagmus in midline medullary lesion. J Neurol 260:2908–
536 2910.

537 Hirai N (1983) Vestibular afferent inputs to lobules I and II of the cerebellar
538 anterior lobe vermis in the cat. Brain Res 277:145–149.

539 Horn AKE, Leigh RJ (2011) The anatomy and physiology of the ocular motor
540 system. In: Handbook of clinical neurology, pp 21–69. Elsevier B.V.

541 Kamath BY, Keller EL (1976) A neurological integrator for the oculomotor
542 control system. Math Biosci 30:341–352.

543 Kaneko CRS (1997) Eye Movement Deficits After Ibotenic Acid Lesions of the
544 Nucleus Prepositus Hypoglossi in Monkeys. I. Saccades and Fixation. J
545 Neurophysiol 78:1753–1768.

546 Kheradmand A, Zee DS (2011) Cerebellum and Ocular Motor Control. Front
547 Neurol 2:1–15.

548 Kim EJ, Juavinett AL, Kyubwa EM, Jacobs MW, Callaway EM (2015) Three
549 Types of Cortical Layer 5 Neurons That Differ in Brain-wide Connectivity
550 and Function. Neuron 88:1253–1267.

551 Kokkoroyannis T, Scudder CA, Balaban CD, Highstein SM, Moschovakis AK
552 (1996) Anatomy and physiology of the primate interstitial nucleus of cajal: I.
553 Efferent projections. J Neurophysiol 75:725–739.

554 Kotchabhakdi N, Walberg F (1978) Cerebellar afferent projections from the
555 vestibular nuclei in the cat: An experimental study with the method of
556 retrograde axonal transport of horseradish peroxidase. Exp Brain Res
557 31:591–604.

Langer T, Fuchs AF, Scudder CA, Chubb MC (1985) Afferents to the flocculus of the cerebellum in the rhesus macaque as revealed by retrograde transport of horseradish peroxidase. J Comp Neurol 235:1–25.

Leigh RJ, Zee DS (2015) The Neurology of Eye Movements. Oxford University Press.

Matsushita M, Okado N (1981) Cells of origin of brainstem afferents to lobules I and II of the cerebellar anterior lobe in the cat. Neuroscience 6:2393–2405.

McCrea RA, Baker R (1985) Anatomical connections of the nucleus prepositus of the cat. J Comp Neurol 237:377–407.

McCrea RA, Horn AKE (2006) Nucleus prepositus. In: Progress in Brain Research, pp 205–230.

Mori T, Morimoto K (2014) Rabies virus glycoprotein variants display different patterns in rabies monosynaptic tracing. Front Neuroanat 7:47.

Moschovakis AK (1997) The neural integrators of the mammalian saccadic system. Front Biosci 2:d552-77.

573 Nagao S, Ito M, Karachot L (1985) Eye field in the cerebellar flocculus of
574 pigmented rabbits determined with local electrical stimulation. Neurosci
575 Res 3:39–51.

576 Nakamagoe K (2000) Evidence for Brainstem Structures Participating in
577 Oculomotor Integration. Science (80-) 288:857–859.

578 Nakamagoe K, Shimizu K, Koganezawa T, Tamaoka A (2012) Downbeat
579 nystagmus due to a paramedian medullary lesion. J Clin Neurosci
580 19:1597–1599.

581 Navarro-López J de D, Alvarado JC, Márquez-Ruiz J, Escudero M, Delgado-
582 García JM, Yajeya J (2004) A cholinergic synaptically triggered event
583 participates in the generation of persistent activity necessary for eye
584 fixation. J Neurosci 24:5109–5118.

585 Navarro-López J de D, Delgado-García JM, Yajeya J (2005) Cooperative
586 glutamatergic and cholinergic mechanisms generate short-term
587 modifications of synaptic effectiveness in prepositus hypoglossi neurons. J
588 Neurosci 25:9902–9906.

589 Osakada F, Callaway EM (2013) Design and generation of recombinant rabies
590 virus vectors. Nat Protoc 8:1583–1601.

591 Paxinos G, Watson C (2018) The Rat Brain in Stereotaxic Coordinates
592 Compact, 7th ed. San Diego: Elsevier Academic Press.

593 Payne JN (1983) Axonal branching in the projections from precerebellar nuclei
594 to the lobulus simplex of the rat's cerebellum investigated by retrograde
595 fluorescent double labeling. J Comp Neurol 213:233–240.

596 Robinson D (1989) Integrating With Neurons. Annu Rev Neurosci 12:33–45.

597 Robinson DA (1974) The effect of cerebellectomy on the cat's vestibulo-ocular
598 integrator. Brain Res 71:195–207.

599 Robinson DA (1975) Oculomotor control signals. In: Basic mechanisms of
600 ocular motility and their clinical implications, pp 337–374. Pergamon.

601 Røste GK (1989) Observations on the projection from the perihypoglossal
602 nuclei to the cerebellar cortex and nuclei in the cat. A retrograde WGA-
603 HRP and fluorescent tracer study. Anat Embryol (Berl) 180:521–533.

Røste GK, Dietrichs E (1988) Demonstration of a sparse direct projection from the interstitial nucleus of Cajal to the cerebellum in the cat. Arch Ital Biol 126:111–118.

Saito Y, Sugimura T (2020) Different Activation Mechanisms of Excitatory Networks in the Rat Oculomotor Integrators for Vertical and Horizontal Gaze Holding. eNeuro 7.

Saito Y, Sugimura T (2023) Serotonergic current responses of neurons in rat oculomotor neural integrators. J Neurophysiol 129:399–409.

Saito Y, Sugimura T, Yanagawa Y (2017) Comparisons of Neuronal and Excitatory Network Properties between the Rat Brainstem Nuclei that Participate in Vertical and Horizontal Gaze Holding. eNeuro 4:1–12.

Saito Y, Yanagawa Y (2010) Synaptic mechanism for the sustained activation of oculomotor integrator circuits in the rat prepositus hypoglossi nucleus: contribution of Ca2+-permeable AMPA receptors. J Neurosci 30:15735–15746.

Sato Y, Kawasaki T (1984) Functional localization in the three floccular zones related to eye movement control in the cat. Brain Res 290:25–31.

621 Sato Y, Kawasaki T (1990) Eye movement evoked by stimulation of Purkinje
622 cell zones of the cerebellar flocculus in the cat. Acta Med Biol 38:27–35.

623 Sato Y, Kawasaki T, Ikarashi K (1983) Afferent projections from the brainstem
624 to the three floccular zones in cats. II. Mossy fiber projections. Brain Res
625 272:37–48.

626 Schindelin J, Arganda-Carreras I, Frise E, Kaynig V, Longair M, Pietzsch T,
627 Preibisch S, Rueden C, Saalfeld S, Schmid B, Tinevez J-Y, White DJ,
628 Hartenstein V, Eliceiri K, Tomancak P, Cardona A (2012) Fiji: an open-
629 source platform for biological-image analysis. Nat Methods 9:676–682.

630 Schonewille M, Luo C, Ruigrok TJH, Voogd J, Schmolesky MT, Rutteman M,
631 Hoebeek FE, De Jeu MTG, De Zeeuw CI (2006) Zonal organization of the
632 mouse flocculus: Physiology, input, and output. J Comp Neurol 497:670–
633 682.

634 Shadmehr R (2017) Distinct neural circuits for control of movement vs. holding
635 still. J Neurophysiol 117:1431–1460.

636 Shemesh AA, Zee DS (2019) Eye Movement Disorders and the Cerebellum. J
637 Clin Neurophysiol 36:405–414.

638 Skavenski AA, Robinson DA (1973) Role of abducens neurons in
639 vestibuloocular reflex. J Neurophysiol 36:724–738.

640 Spence SJ, Saint-Cyr JA (1988a) Comparative topography of projections from
641 the mesodiencephalic junction to the inferior olive, vestibular nuclei, and
642 upper cervical cord in the cat. J Comp Neurol 268:357–374.

643 Spence SJ, Saint-Cyr JA (1988b) Mesodiencephalic projections to the
644 vestibular complex in the cat. J Comp Neurol 268:375–388.

645 Sugihara I, Ebata S, Shinoda Y (2004) Functional Compartmentalization in the
646 Flocculus and the Ventral Dentate and Dorsal Group y Nuclei: An Analysis
647 of Single Olivocerebellar Axonal Morphology. J Comp Neurol 470:113–133.

648 Sugihara I, Shinoda Y (2004) Molecular, Topographic, and Functional
649 Organization of the Cerebellar Cortex: A Study with Combined Aldolase C
650 and Olivocerebellar Labeling. J Neurosci 24:8771–8785.

651 Sugimura T, Saito Y (2021) Distinct proportions of cholinergic neurons in the rat
652 prepositus hypoglossi nucleus according to their cerebellar projection
653 targets. J Comp Neurol 529:1541–1552.

654 Tan J, Gerrits NM, Nanhoe R, Simpson JI, Voogd J (1995) Zonal organization
655 of the climbing fiber projection to the flocculus and nodulus of the rabbit: A
656 combined axonal tracing and acetylcholinesterase histochemical study. J
657 Comp Neurol 356:23–50.

658 Tian J, Otero-Millan J, Zee DS, Kheradmand A (2023) Upbeat Nystagmus with
659 an Unusual Velocity-Decreasing and Increasing Waveform: a Sign of Gaze-
660 Holding Dysfunction in the Paramedian Tracts in the Medulla? Cerebellum
661 22:148–154.

662 Tomlinson RD, Robinson DA (1984) Signals in vestibular nucleus mediating
663 vertical eye movements in the monkey. J Neurophysiol 51:1121–1136.

664 Voogd J, Wylie DRW (2004) Functional and anatomical organization of floccular
665 zones: A preserved feature in vertebrates. J Comp Neurol 470:107–112.

666 Zee DS, Leigh RJ, Mathieu-Millaire F (1980) Cerebellar control of ocular gaze
667 stability. Ann Neurol 7:37–40.

668 Zee DS, Yamazaki A, Butler PH, Gücer G (1981) Effects of ablation of flocculus
669 and paraflocculus of eye movements in primate. J Neurophysiol 46:878–
670 899.

671 Zhang Y, Kaneko R, Yanagawa Y, Saito Y (2014) The vestibulo- and prepositо-
672 cerebellar cholinergic neurons of a ChAT-tdTomato transgenic rat exhibit
673 heterogeneous firing properties and the expression of various
674 neurotransmitter receptors. Eur J Neurosci 39:1294–1313.

675 Zhang Y, Yanagawa Y, Saito Y (2016) Nicotinic acetylcholine receptor-
676 mediated responses in medial vestibular and prepositus hypoglossi nuclei
677 neurons showing distinct neurotransmitter phenotypes. J Neurophysiol
678 115:2649–2657.

679 Zhang Y, Yanagawa Y, Saito Y (2018) Firing responses mediated via distinct
680 nicotinic acetylcholine receptor subtypes in rat prepositus hypoglossi nuclei
681 neurons. J Neurophysiol 120:1525–1533.

682

683

684 **Figure legends**

685 **Figure 1. Neurons retrogradely labeled via tracer injection into the**
686 **vestibulocerebellum.**

(a1, b1) Schematic drawings of the injection of dextran-conjugated Alexa 488 into the FL (a1) and UN (b1) of rats. (a2, b2) Fluorescence photomicrographs of the injection sites. Each photo is separated by 300 μm in the rostrocaudal direction. (a3, b3) Confocal images of frontal sections that include the PHN. The dashed line approximately indicates the boundary of the PHN. (a4, b4) Enlarged images of the box in (3). (a5, b5) Fluorescence photomicrographs of frontal sections that include the inferior olive. (a6, b6) Confocal images of frontal sections that include the INC. The dashed line approximately indicates the boundary of the INC. (a7, b7) Enlarged images of the box in (6). Scale bars: (a2, b2) 500 μm; (a3-7, b3-7) 100 μm. 4 V, fourth ventricle; FL, flocculus; UN, uvula and nodulus; r-MAO, rostral part of the medial accessory olive; beta, subnucleus beta of the inferior olive. The Roman numerals indicate the cerebellar lobules.

Figure 2. Neurons retrogradely labeled following tracer injection into lobules Ⅰ-Ⅱ in the vermis and crus Ⅰ-Ⅱ.

(a1, b1) Schematic drawings of the injection of dextran-conjugated Alexa 488 into lobules Ⅰ-Ⅱ in the vermis (a1) and crus Ⅰ-Ⅱ (b1) of rats. (a2, b2) Fluorescence photomicrographs of the injection sites. Each photo is separated by 300 μm in

the rostrocaudal direction. (a3, b3) Fluorescence photomicrographs of frontal sections that include the PHN. The dashed line approximately indicates the boundary of the PHN. (a4, b4) Enlarged images of the box in (3). (a5, b5) Fluorescence photomicrographs of frontal sections that include the inferior olive. (a6, b6) Brightfield images of frontal sections that include the INC. The dashed line approximately indicates the boundary of the INC. (a7, b7) Enlarged fluorescence images of the box in (6). Scale bars: (a2, b2) 500 μm; (a3-7, b3-7) 100 μm. 4 V, fourth ventricle. c-MAO, caudal part of the medial accessory olive; v-PO, ventral lamella of the principal olive; d-PO, dorsal lamella of the principal olive. The Roman numerals indicate the cerebellar lobules.

Figure 3. Indirect connections from the INC to the VC via the PHN and MVN. (a) Experimental design of retrograde monosynaptic tracing from the PHN and MVN projecting to the FL or UN of a rat. (b1, c1) Fluorescence photomicrographs of GFP at the sites of injection of two helper AAV2retro viruses (AAV2retro-G and AAV2retro-GFP-TVA) on the right side of the FL (b1) and the midline region of the UN (c1). (b2-3, c2) Example of starter cells (arrows) in the right PHN and MVN expressing both GFP and RFP. EnvA-RVdG-RFP was injected into the right

side of the PHN and MVN. (b4, c3) Examples of RFP-expressing neurons in the INC that received retrograde transsynaptic infection with rabies virus from starter cells. (d1-2) Numbers of starter cells in the PHN and MVN (1) and RFP-expressing neurons in the INC (2), which provide inputs to the starter cells, for each rat analyzed. “FL” and “UN” represent groups where helper AAVs were injected into the FL and UN, respectively. The numbers following “FL” and “UN” are used to distinguish individual rats within each group. (d3) Relationships between the number of starter cells and RFP-expressing neurons in the INC. Scale bars: (b1, c1) 500 μm; (b2-4, c2-3) 100 μm.

Figure 4. Control experiments for rabies transsynaptic tracing.

(a) Frontal section of the cerebellum at the site of injection of AAV2retro-GFP-TVA in the UN (AAV2retro-G was not injected). (b) Enlarged image of the box in (a). (c) Frontal section showing the PHN and MVN after AAV2retro-GFP-TVA injection into the UN and after EnvA-RVdG-RFP injection into the PHN and MVN. The dashed line approximately indicates the boundary of the PHN and MVN. (d, e) RFP (d) and GFP (e) images from (c). The arrows indicate neurons that express both GFP and RFP. Scale bars: (a, b) 500 μm; (e) 100 μm.

Figure 5. Distribution of RFP-expressing neurons in the rostral–caudal regions of the INC.

(a1-3, b1-3) Fluorescence photomicrographs of frontal sections that include the INC after rabies virus transsynaptic tracing (related to Figure 3). RFP-expressing neurons in the rostral (1), intermediate (2), and caudal (3) regions of the INC following injection of the two helper AAV2 retroviral vectors into the FL (a) and UN (b). (a4, b4) Comparison of the percentages of RFP-expressing (RFP+) neurons in each region with respect to the total number of RFP-expressing neurons in the INC (a4, n = 3; b4, n = 4). Individual plots indicate data obtained from individual rats. The error bars represent the SDs. Scale bars: (a3, b3) 100 μm. Asterisks indicate a significant difference between groups (*p < .05; **p < .01).

Figure 6. The indirect INC-FL pathway is mediated via the bilateral PHNs and MVNs.

(a1) Fluorescence photomicrograph of GFP at the site of injection of the two helper AAV2retro viruses (AAV2retro-G and AAV2retro-GFP-TVA) on the right of

759 the FL. (a2-3) Example starter cells (arrows) expressing both GFP and RFP in
760 the left PHN and MVN. EnvA-RVdG-RFP was injected into the left PHN and MVN.
761 Figure 3 shows that the rabies virus was injected into the right PHN and MVN.
762 (a4-5) Fluorescence photomicrographs of frontal sections that include the INC.
763 RFP-expressing neurons, which received retrograde transsynaptic infection with
764 rabies virus from starter cells, were observed in the right (4) and left INC (5). (b)
765 Schematic diagram of the pathway from the INC to the FL via the bilateral PHNs
766 and MVNs revealed in this study. The diagram shows the neural pathway to the
767 right FL only. Scale bars: (a1) 200 μm; (a2-5) 100 μm.
768

769 **Figure 7. Inferior olive neurons retrogradely labeled following helper AAV2**
770 **retrovirus injection into the FL.**

771 (a) Fluorescence photomicrographs at the sites of injection of the two helper
772 AAV2 retroviral vectors (AAV2retro-GFP-TVA and AAV2retro-G) in the right FL
773 (related to Figure 3). Each photo is separated by 300 μm in the rostrocaudal
774 direction. (b-d) Fluorescence photomicrographs of frontal sections that include
775 the CDC and VLO of the inferior olive and the r-MAO. The arrows indicate the
776 midline. Scale bars: (a) 200 μm; (b-d) 100 μm. FL, flocculus; CDC, caudal

777 dorsal cap; VLO, ventrolateral outgrowth; r-MAO, rostral part of the medial

778 accessory olive

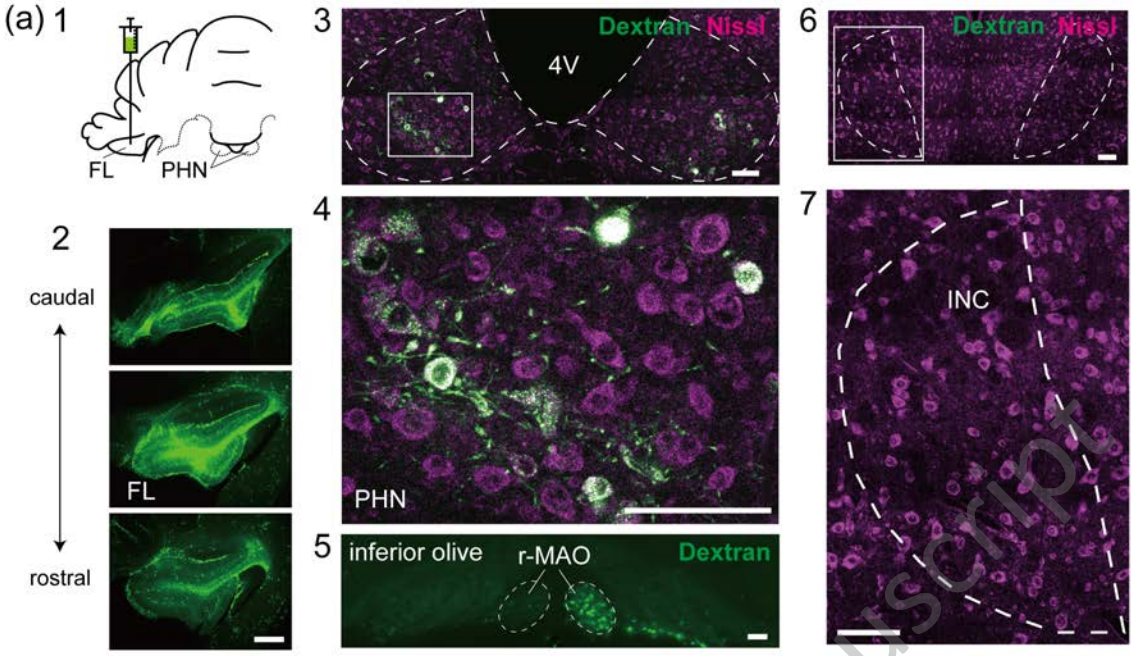

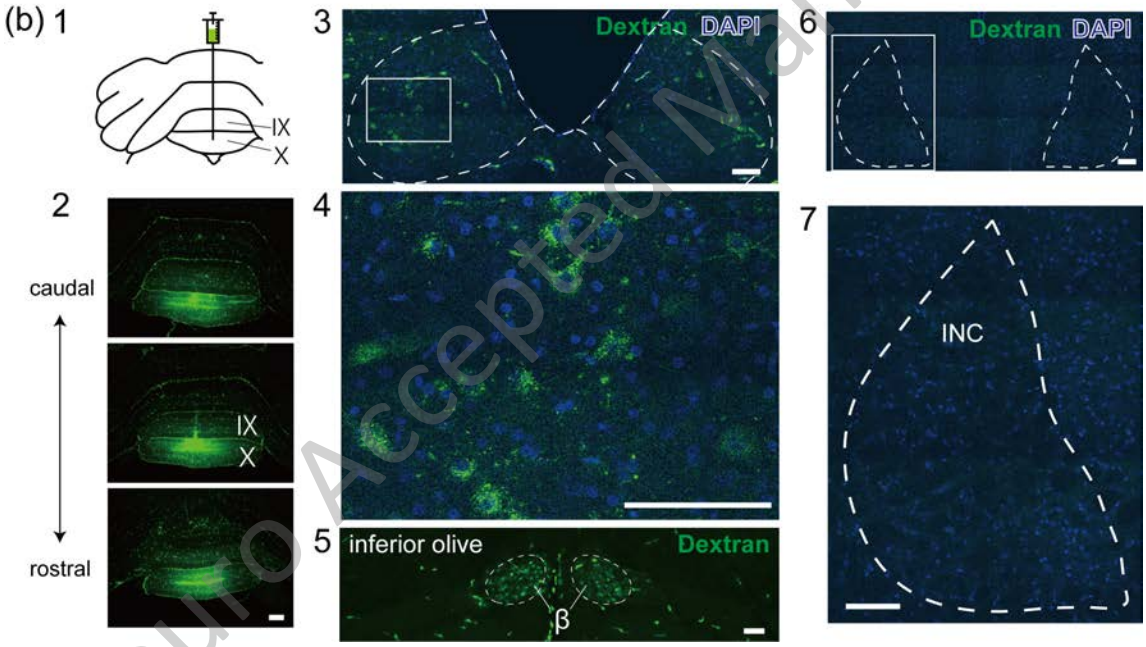

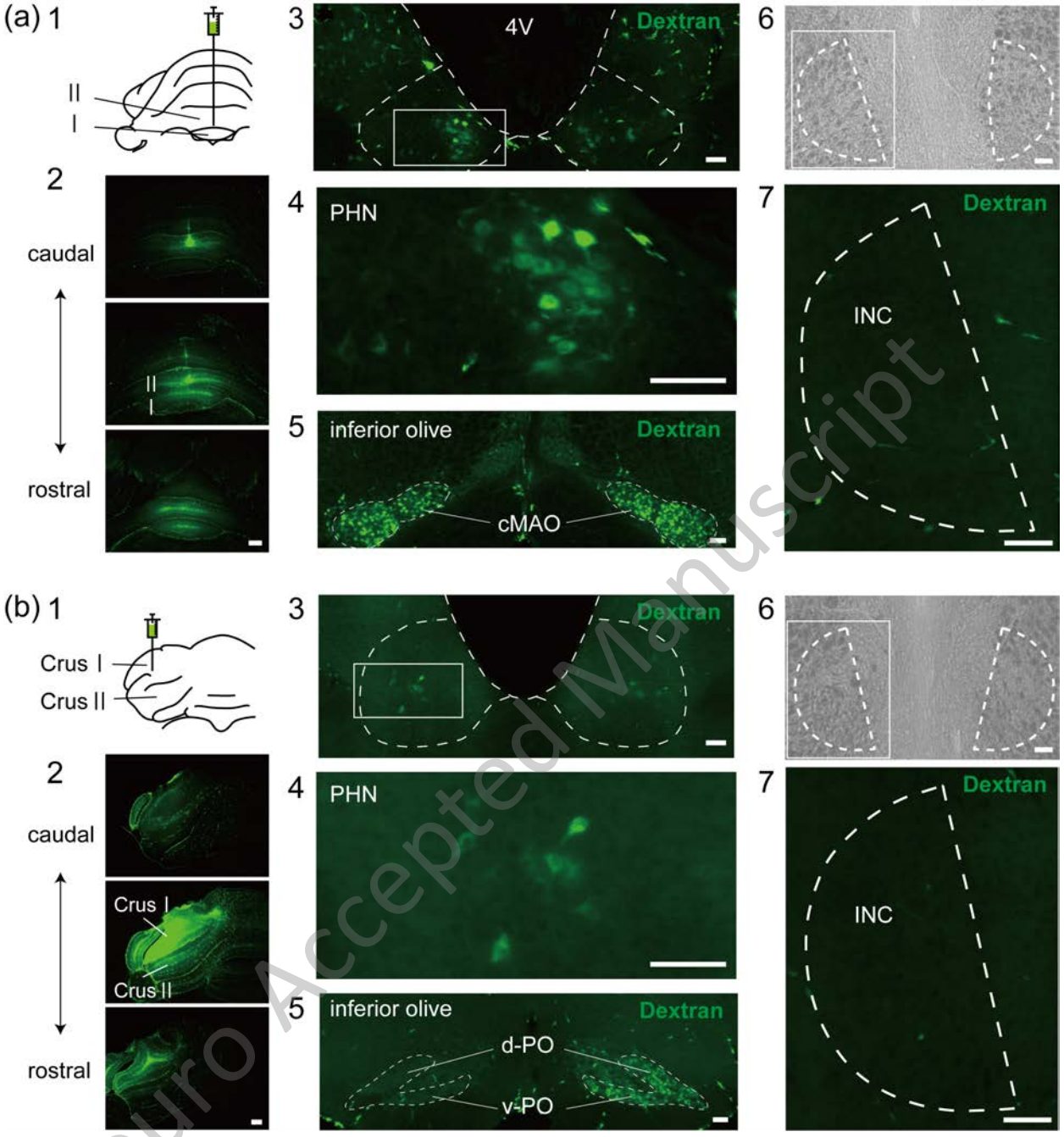

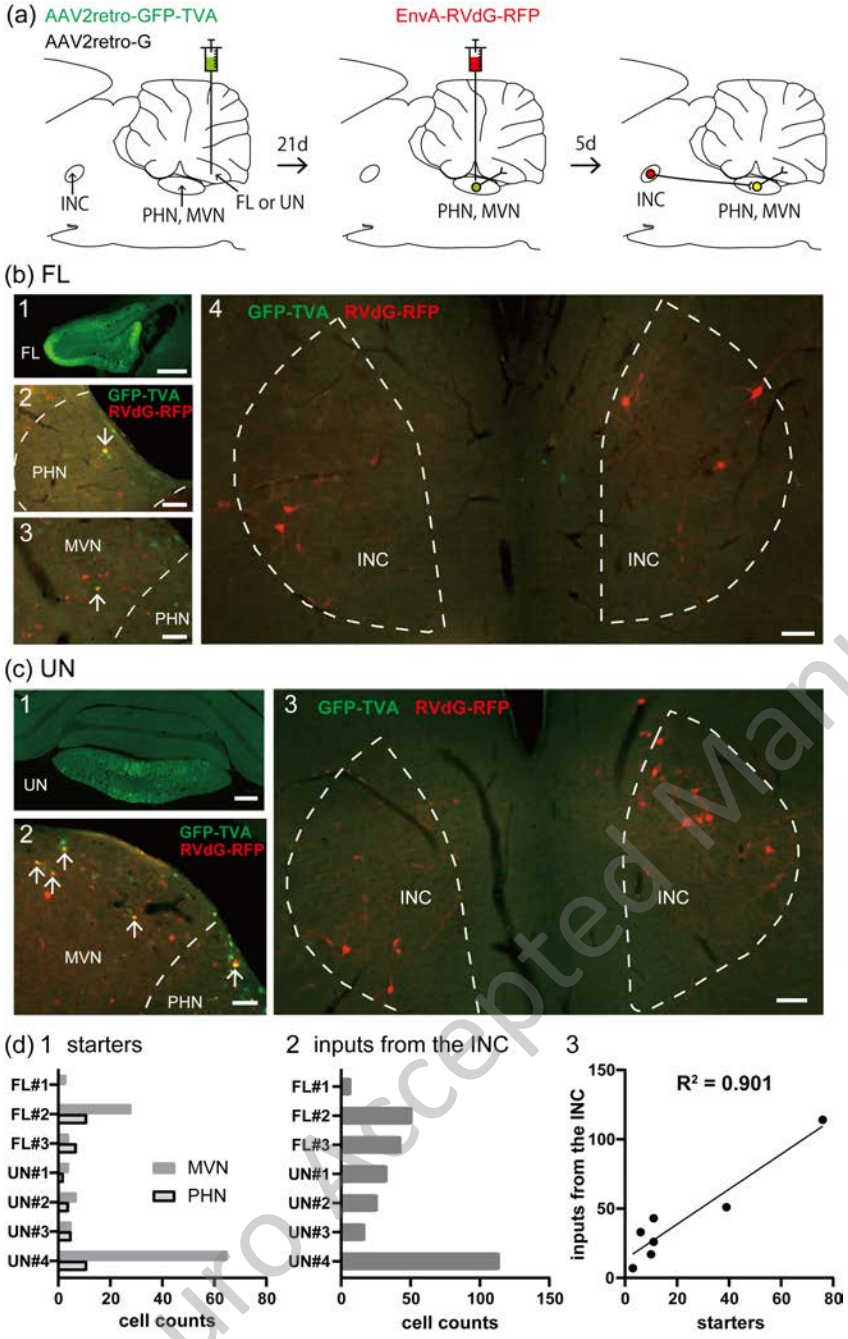

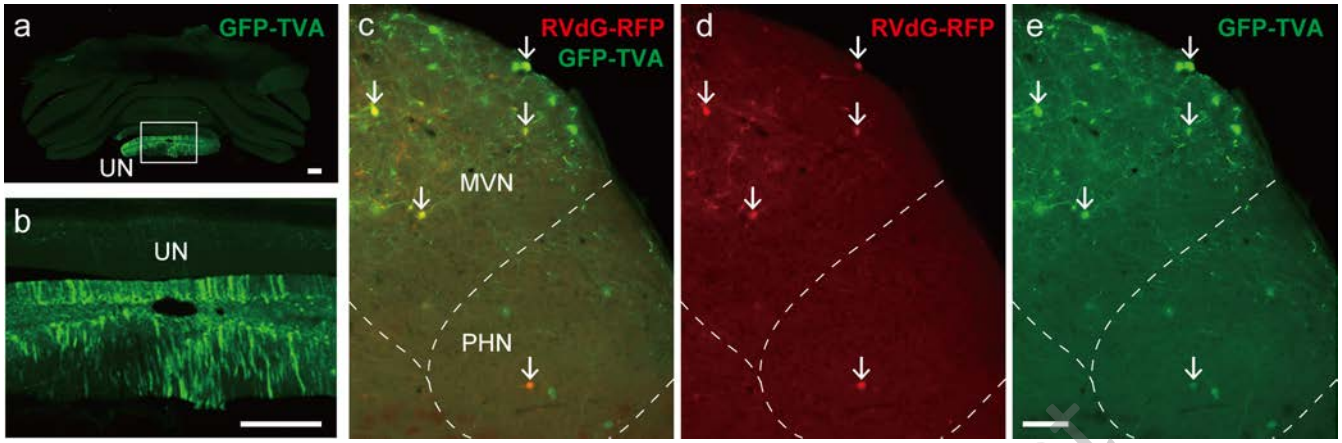

(a) FL

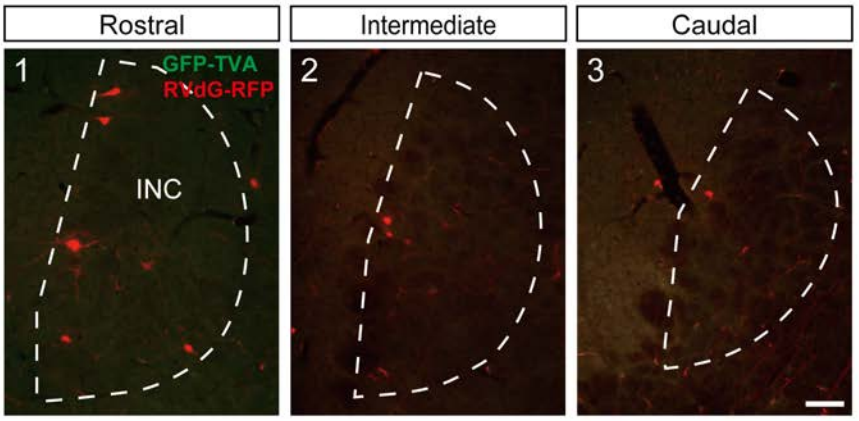

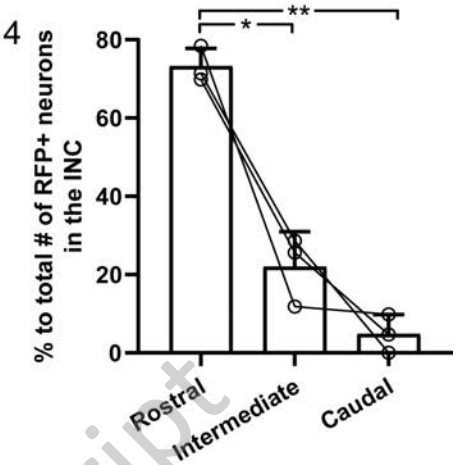

(b) UN